Published in final edited form as:
Biomacromolecules. 2014 October 13; 15(10): 3817–3826. doi:10.1021/bm501156v.

Tailored Freestanding Multilayered Membranes based on Chitosan and Alginate

Joana M. Silva[†,‡], **Ana Rita C. Duarte**[†,‡], **Sofia G. Caridade**[†,‡], **Catherine Picart**[§,‖], **Rui L. Reis**[†,‡], and **João F. Mano**[*,†,‡]

[†]3B's Research Group - Biomaterials, Biodegradables and Biomimetics, University of Minho, Headquarters of the European Institute of Excellence on Tissue Engineering and Regenerative Medicine, AvePark, 4806-909 Taipas, Guimarães, Portugal

[‡]ICVS/3B's - PT Government Associate Laboratory, Braga/Guimarães, Portugal

[§]CNRS, UMR 5628, LMGP, F-38016, Grenoble, France

[‖]University Grenoble Alpes, Institut National Polytechnique de Grenoble, F-38016 Grenoble, France

Abstract

Engineering metabolically demanding tissues requires the supply of nutrients, oxygen and removal of metabolic byproducts, as well as adequate mechanical properties. In this work, we propose the development of chitosan (CHIT) / alginate (ALG) freestanding membranes fabricated by layer-by-layer (LbL). CHIT/ALG membranes were cross-linked with genipin at a concentration of 1 $mg.mL^{-1}$ or 5 $mg.mL^{-1}$. Mass transport properties of glucose and oxygen were evaluated on the freestanding membranes. The diffusion of glucose and oxygen decreases with increasing cross-linking concentration. Mechanical properties were also evaluated in physiological–simulated conditions. Increasing cross-linking density leads to an increase of storage modulus, Young modulus and ultimate tensile strength, but to a decrease in the maximum hydrostatic pressure. The *in vitro* biological performance demonstrates that cross-linked films are more favorable for cell adhesion. This work demonstrates the versatility and feasibility of LbL to generate nanostructured constructs with tunable permeability, mechanical and biological properties.

Keywords

Biomimetic; Tissue engineering; relaxation behavior; dynamic mechanical analysis

Introduction

Among the different surface engineering methods, the layer-by-layer (LbL) assembly has emerged as a powerful tool to create advanced materials with nanometer and micrometer-scale control 1, 2. Introduced 20 years ago by *Moehwald*, *Decher* and co-workers, the

[*]Corresponding author. jmano@dep.uminho.pt.

Europe PMC Funders Author Manuscripts

principle of LbL most of the time relies on the build-up of polyelectrolyte multilayer (PEMs) films through stepwise deposition of oppositely charged polyelectrolytes 2–4.

The procedure is very versatile and enables the use of different charged species, including biological molecules (proteins, polysaccharides, viruses and DNA) and various kind of nanoparticles 2, 4–6. Among the polysaccharides that have been used, chitosan (CHIT) and alginate (ALG) received particular attention due to their potential in LbL, stability in physiological conditions and also their biocompatibility 7–10. Besides the nature of polyelectrolytes other processing parameters can be adjusted to tailor the morphology, internal molecular structure, thickness, swelling ability, diffusion of molecules and mechanical properties 11. With the simple adjustment of molecular weight, temperature, charge density, polyelectrolyte concentration, pH, chemical or photo cross-linking and ionic strength an infinite variety of architectures can be produced 2–4, 12–15. In terms of substrates, distinct templates may be employed to obtain complex structures only based on polyelectrolyte multilayers (PEMs). The release of thin PEMs from a solid substrate to a freestanding state has opened the door to boost the development of innovative materials such as: capsules 16, 17, membranes 18, 19, hollow tubes 20 or porous scaffolds 21, 22. The advantage of freestanding films from PEM rather than other freestanding film production is based on the tremendous advantage to create macroscopic structures only based on nanostratified multilayers 4, 23. This bottom-up procedure enables the fine control of nanoscale films. Thus, freestanding films obtained from polyelectrolyte multilayer are a much simpler, cost-effective, flexible, and versatile approach for fabricating robust multilayer assemblies, surpassing several limitation imposed by the former techniques 15, 24. In general, the techniques for producing freestanding films include the presence of sacrificial layers, the dissolution of initial layers and the neutralization of charged layers 18. However, these approaches are likely to induce defects and increase the surface roughness into the PEMs 18, 25. Freestanding multilayers have been mostly focused on synthetic or nanocomposite films. Studies on films entirely made of polysaccharides are still scarce18, 25. In this work, CHIT and ALG freestanding membranes were used as a model which allows the future transposition of these PEMs to more complex structures. Freestanding membranes were produced by simple detachment of an underlying polypropylene support, as previously reported 25. However, CHIT/ALG PEMs are commonly reported to exhibit low stiffness and poor cell adhesion, presenting low stability at physiological conditions 7, 26. Genipin is a natural product extracted from the gardenia fruit, which may help to overcome these drawbacks on PEMs 7, 26, 27. The main aim of this work is to study the potential of CHIT/ALG freestanding membranes with or without cross-linking for tissue engineering (TE) applications. This will involve the characterization of the diffusion of basic compounds such as glucose and oxygen. Moreover, the effect of cross-linking with genipin on both mechanical and biological properties will also be evaluated.

Materials and Methods

Production of freestanding membranes

The two polyelectrolytes used to process the multilayers were CHIT medium molecular weight (M_W 190.000-310.000 Da, 82.6 % degree of deacetylation, ref. 448877, Sigma

Aldrich, USA) and low viscosity ALG (538 kDa, ≈ 250 cp, ref. 71238, Sigma Aldrich, USA). Chitosan was purified by a series of filtration and precipitation in water and ethanol steps. The polyelectrolyte solutions were freshly prepared at a concentration of 0.2 % (w/v). For the adjustment of pH, a sodium acetate buffer (0.1M) was prepared at pH 5.5 in the presence of additional salt (0.15 M NaCl).

Freestanding membranes were produced using a polypropylene support previously washed in ethanol and water. Polyelectrolytes solutions were alternately deposited on the template to form 100 bilayers (dL) of CHIT and ALG, using a dipping robot especially designed for the automatic fabrication of multilayers. Between each polyelectrolyte solution the templates were immersed on acetate buffer solution. After drying at room temperature, the membranes could be easily detached from the flat substrate. Cross-linking of freestanding films was performed with genipin (Wako chemical, USA). A genipin solution (1 or 5 $mg.mL^{-1}$) was prepared by dissolving the adequate amount of lyophilized genipin into a dimethyl sulfoxide (Sigma Aldrich, USA)/sodium acetate buffer (0.15 M NaCl, pH 5.5) mixture (1:4 (v/v)). The crosslinking agent solution was incubated with membranes overnight. Afterwards, the membranes were extensively washed with ethanol to dissolve the amount of genipin that did not react and dried at 37 °C.

Scanning Electron Microscopy (SEM)

The morphology of the freestanding membranes was observed by Scanning Electron Microscopy (SEM), using a Leica Cambridge S 360 (UK) operated at 15 kV accelerating voltage. All the samples were sputtered with a conductive gold layer, using a sputter coater SC502 (Fison instruments, UK). For the cross section observation, the detached freestanding were immersed in liquid nitrogen until free fracture. Three freestanding membranes were measured for each condition.

Atomic Force Microscopy (AFM) Imaging

Dried freestanding membranes were imaged using a MultiMode STM microscope controlled by the NanoScope III from Digital Instruments system (Bruker, France) operating in intermittent contact mode. A ScanAsyst-Air cantilever (Bruker, France) with a resonance frequency of 320 kHz and a spring constant of 2 N/m was used. Substrate topographies were imaged with 512 × 512 $pixels^2$ at line rates of 1 Hz. For surface roughness analysis, 5 × 5 μm^2 AFM images were obtained and the root means squared roughness (R_{RMS}) and average height value (H_{av}) from the principal x−y plane was calculated. The analysis of the images was performed using Gwydion. At least three measurements were performed in different specimens.

Fluorometric Measurements

The kinetics of CHIT/ALG multilayers cross-linking with genipin was measured by fluorescence. Thus, $(CHIT/ALG)_{10}$-CHIT multilayers were prepared in 96-well tissue plate. The coatings were incubated in genipin solution for defined durations (1h, 3h, 6h, 9h and 12h). At predetermined time points the fluorescence intensity of the coatings were measured with a microplate reader (Synergy HT, Bio-TEK, USA) using 590 and 645 nm as excitation and emission wavelengths, respectively, as previously reported 28.

Cross-linking degree analysis

The cross-linking of PEMs with genipin was evaluated using the trypan blue method which has affinity to free amines 29–31. The test was performed by immersing the non-cross-linked and the cross-linked membranes in trypan blue 0.4% (Invitrogen, USA) diluted 50x in acetate buffer (0.15 M NaCl, pH 5.5) overnight at 37º C. The absorbance of the supernatant was measured at 580 nm in a microplate reader (Synergy HT, Bio-TEK, USA). A standard curve was prepared by measuring the absorbance for a series of trypan blue solution at different concentrations. The cross-linking degree was calculated as follows (equation 1):

$$CL\,(\%) = \frac{\left(NH_3^+ non-cross-linked\, membranes\right) - \left(NH_3^+ cross-linked\, membranes\right)}{NH_3^+ non-cross-linked\, membranes} \quad (1)$$

Mechanical Tests

The dynamic mechanical analysis (DMA) measurements were performed using a TRITEC8000B DMA (Trinton Technology, UK). Freestanding membranes were immersed in PBS until equilibrium was reached (overnight). Samples were tested at physiological-like conditions, i.e. immersed in PBS at 37ºC placed in a Teflon® reservoir. The distance between the clamps was 10 mm and the membranes were cut with about 5.5 mm of width and 50 mm of length. The thickness of the membranes were 76 ± 0.7 μm, 56 ± 0.3 μm and 48 ± 0.4 μm in thickness for CHIT/ALG membranes, cross-linked membranes at 1 and 5 $mg.mL^{-1}$, respectively. After measuring the geometry the samples were clamped in the DMA apparatus and immersed in the PBS bath. Tensile experiments were carried out following cycles of increasing frequency ranging from 0.1 to 20 Hz, with constant strain amplitude of 30 μm. Three samples were used per condition.

The mechanical properties of freestanding membranes were also studied in wet state using an INSTRON 5540 (Instron Int. Ltd, High Wycombe, UK) universal testing machine with a load cell of 1 kN. The data presented is the average of at least 3 measurements. The dimensions of the specimens used were 60 mm in length, 6.5 mm width and 76 ± 0.7 μm, 56 ± 0.3 μm and 48 ± 0.4 μm in thickness for CHIT/ALG membranes, cross-linked membranes at 1 and 5 $mg.mL^{-1}$, respectively. The load was placed midway between the supports with a span (L) of 20 mm. The crosshead speed was 5 mm min^{-1}. For each condition the specimens were loaded until core break.

The burst strength was determined using a home-made apparatus. Briefly, freestanding membranes were immersed in PBS until equilibrium was reached. Samples were placed into the apparatus (syringe previously cut (A= 3.14 cm^2)) and sealed at the circumference to prevent leaking. PBS was added in the apparatus and a load applied on plunger of the syringe was also gradually increased until the apparition of a leak. The rupture was monitored and recorded using a universal mechanical testing machine.

Europe PMC Funders Author Manuscripts

Water-uptake

The water-uptake ability of the freestanding films was measured soaking dry films of known weight in PBS (Sigma, USA) at 37°C. The swollen films were removed after 12 hours. After removing the excess of PBS using a filter paper (Filter Lab, Spain), the freestanding films were weighed with an analytical balance (Denver Instrument, Germany). The water uptake was calculated as followed:

$$Water\ uptake\% = \frac{W_w - W_d}{W_d} \times 100 \quad (2)$$

where W_w and W_d are the weights of swollen and dried freestanding films, respectively.

Permeability to Glucose and Oxygen

The permeability measurements were conducted using a glass Franz-type diffusion cell (PermeGear) with a 8 mL reactor compartment (effective mass transfer area of 1 cm^2). The membranes were previously equilibrated in a PBS solution (overnight), placed between the two compartments and hold with a stainless steel clamp. The receptor compartment was immediately filled with PBS solution and air bubbles were removed. Finally, the donor compartment was filled with 5 $mg.mL^{-1}$ of glucose (PBS, pH 7.4) (Sigma Aldrich, USA). Aliquots of 200 μL were withdrawn from the receptor compartment at predetermined time periods and replenished by fresh PBS. The experiments were performed at 37°C and the receptor compartment was stirred at 400–600 rpm using a magnetic bar to eliminate the boundary layer effect. The time-dependent concentration of glucose in the receptor chamber was assessed by the dinitrosalicylic acid (DNS) method. The DNS reacts with reducing sugars, and other reducing molecules, forming 3-amino-5-nitrosalicylic acid, an aromatic compound that strongly absorbs light at 540 nm, therefore allowing a quantitative spectrophotometric measurement of the amount of reducing sugar present 32. The amount of glucose was measured by absorbance at a wavelength of 540 nm using a microplate reader (Synergy HT, Bio-TEK, USA).

The oxygen permeability measurements were conducted using a container with a 200 mL reactor compartment (effective mass transfer area of 1.3 cm^2). The membranes were previously equilibrated in a PBS solution overnight and placed between the two compartments. The receptor compartment was filled with PBS solution and all the oxygen was removed by purge with nitrogen. Finally, in the donor compartment a continuous flow of air was applied 6 SCFH (20 SCFH flow meter). The experiments were performed at 37°C and the receptor compartment was stirred at 400–600 rpm using a magnetic bar. The time-dependent concentration of oxygen in the receptor chamber was determined using a CellOx 325 probe (WTW, Germany). The probe was sealed inside the receptor chamber where the oxygen concentration was recorded at each 10 minutes.

In both cases the permeability (P) of glucose and oxygen was calculated by the following equation (equation 3) 33:

$$-ln\left(1-\frac{2C_t}{C_0}\right)=\frac{2A}{V}\times P\times t \quad (3)$$

Where C_t is the concentration in the receptor compartment at time t, C_0 is the initial concentration in the donor compartment, V is the solution volume in the two compartments, and A is the effective area of permeation. The permeability coefficient can be calculated from the slope of the curve - ($V/2A$)·ln ($1-2C_t/C_0$) *versus t*.

The diffusion coefficient (D) of solutes across the membrane was calculated according to Fick's law of diffusion, as follows (equation 4) 34:

$$D=\frac{V_1V_2}{V_1+V_2}\times\frac{h}{A}\times\frac{1}{t}ln\left(\frac{C_f-C_i}{C_f-C_t}\right) \quad (4)$$

Where D is the diffusion coefficient ($cm^2.s^{-1}$); C_i and C_f are the initial and final concentrations and C_t is the concentration at time t of solute in the receptor side, respectively ($mol.L^{-1}$); V_1 and V_2 correspond to the volume of the liquid in the donor compartment and that in the receptor compartment (cm^3), respectively; h is the thickness of the membrane (cm); and A is the effective diffusion area of the membrane (cm^2).

The partition coefficient (K_d) is defined as a measure of the solubility of the solute in the membrane. The partition coefficient for the system was calculated as follows (equation 5) 33, 35

$$K_d=\frac{P\times h}{D} \quad (5)$$

Where P is the permeability, h is the thickness of the membrane and D is the diffusion coefficient.

Cellular Tests

To evaluate the biological performance of CHIT/ALG and cross-linked CHIT/ALG freestanding membranes, cell culture studies were performed with L929, a mouse fibroblast of connective tissue cell line (European Collection of Cell Cultures (ECCC), UK). Cells were cultured in Dulbecco's modified Eagle's medium (DMEM; Sigma, USA), supplemented by 10% heat-inactivated fetal bovine serum (FBS; Biochrom AG, Germany) and 1% antibiotic- antimicotic (Gibco, USA). Prior to cell seeding (50 000 cells per well), membranes were sterilized with 70% (v/v) ethanol overnight and then rinsed three times in PBS. CHIT/ALG and cross-linked CHIT/ALG freestanding membranes were incubated for 1 and 3 days at 37ºC in a humidified 5% CO_2 atmosphere. 4,6-Diaminidino-2-phenylindole-dilactate (DAPI, 20 $mg.mL^{-1}$, Sigma-Aldrich, USA) and phalloidintetramethylrhodamine B isothiocyanate dyes (phalloidin, 10 $mg.mL^{-1}$, Sigma-Aldrich, USA) were used to perform a

Europe PMC Funders Author Manuscripts

DAPI–phalloidin assay (n= 5 samples per well, in triplicate). Briefly at each time point, culture medium was removed and the samples fixed in 10% formalin. After 1 hour, formalin was removed and replaced by PBS. Upon PBS washing, 1 mL of PBS containing 10 μL of phalloidin was added for 40 minutes at room temperature and protected from light. After extensively washing, samples were stained with 1 μl of DAPI in 1mL of PBS for 10 minutes. After DAPI staining samples were washed three times with PBS and visualized in the dark by inverted fluorescent microscope (Zeiss, Germany). The cell density and percentage of adherent cells were evaluated by Image J.

Statistical analysis

The experiments were carried out in triplicate otherwise specified. The results were presented as mean ± standard deviation (SD). Statistical analysis was performed by Shapiro Wilk normality test using Graph Pad Prism 5.0 for Windows. After this analysis, non-parametric (Kruskal Wallis test) or parametric tests (one way Anova followed by Turkey test) were used depending if the samples were from normally distributed populations or not, respectively.

Results and Discussion

Morphology and Topography

CHIT and ALG were sequential adsorbed on the surface of hydrophobic polypropylene substrates. The PEMs were easily detached from the substrate due to weak nature of forces between the initial layer (CHIT) and the substrate (Supporting Information Figure S1A). With 100 bilayers, the membranes were found to be robust and easy to handle (Supporting Information Figure S1B and Figure S1C).

The morphology of the freestanding membranes was evaluated by scanning electronic microscopy (SEM) (Figure 1). The results reveal a homogeneous deposition of multilayers along the surface with a dry thickness of 29.3 ± 5.5 μm. Since, one important feature of freestanding membranes is their stability when exposed to aqueous solutions, the films were cross-linked with genipin using two different concentrations 1 $mg.mL^{-1}$ and 5 $mg.mL^{-1}$.The cross-linked membranes at both concentrations present a similar morphology to that observed for the native membrane. The thickness of both cross-linked freestanding membranes was also determined. The dry thickness the CHIT/ALG membranes is 31.3 ± 4.7 μm and 33.1 ± 3.6 μm for a genipin concentration of 1 $mg.mL^{-1}$ and 5 $mg.mL^{-1}$, respectively. Thus, the thickness did not change significantly between the native and the cross-linked films. These results are in concordance with earlier studies where the cross-linking only limits polyelectrolyte diffusion inside the bulk structure and increase its stiffness without significant changes of PEMs thickness in the dry state 36, 37.

The surface topography of un-modified and cross-linked PEMs was analyzed by AFM imaging in intermittent contact mode (Figure 2A). Native and cross-linked freestanding membranes exhibit rough surfaces, represented by sub-micrometer sized outer islets of material uniformly distributed over the surface. The R_{RMS} and H_{av} values are shown in Figure 2B and Figure 2C, respectively. The results reveal that all the freestanding

membranes formulations present a roughness in the order of 70-100 nm and an average height value between 280-380 nm. However, the cross-linking seems to create more uniforms films with reduced roughness.

Cross-linking degree

To determine the extent of cross-linking reactions on CHIT/ALG membranes, trypan blue assays were performed. Trypan blue is a large oligoanionic dye with ability to bind to free amines, leading to a decrease in the blue color intensity of the supernatant solution, which is proportional to the free amines added29–31. Using this principle, CHIT/ALG and cross-linked membranes were incubated in trypan blue solution and the absorbance of the supernatant was measured. As expected, the absorbance of the supernatant increases with higher cross-linked membranes, since the content of free amine groups also decrease (Supporting Information Figure S2). On the other side, the color of membranes presents an opposite behavior, since the blue color was enhanced with higher content of free amines. The intensity of blue color presented by freestanding membranes when immersed in trypan blue is also an alternative method to measure the cross-linking degree. However, in common UV-vis spectrophotometer the signal was saturated. The color change of membranes upon genipin reaction also confirms an efficient cross-linking within the PEMs. After cross-linking with genipin, opaque samples acquire a greenish color due to a covalent coupling with amino groups 28. Variations in fluorescence intensity within the PEMs due to the genipin cross-linking were also evaluated to study the kinetic of the cross-linking reaction (Figure 3A). PEMs cross-linked with genipin emit fluorescence at 630-640 nm when excited at 590 nm. This behavior was already reported for other normally opaque nonfluorescing materials that turn blue and emit a red fluorescence when cross-linked with genipin 27, 28, 38. In this experience, time-dependence fluorescence intensity was evaluated for distinct cross-linking regimens - no crosslinking, cross-linking at 1 $mg.mL^{-1}$ and 5 $mg.mL^{-1}$ for 12 h. At a genipin concentration of 5 $mg.mL^{-1}$ fluorescence intensity is considerable higher when compared with the cross-linking performed at 1 $mg.mL^{-1}$. In both cases the intensity of fluorescence increases along the time. However, after 12 hours the increase in fluorescence intensity of PEMs cross-linked with 1 $mg.mL^{-1}$ was higher than with 5 $mg.mL^{-1}$. This behavior can be explained by the differences in terms of concentration since the concentrations were significantly different. Thus for the same amount of free amines in PEMs the solution with a concentration of 5 $mg.mL^{-1}$ will be a cross-linking most effective reaching the equilibrium faster. Besides this difference, it cannot be assumed that the cross-linking is inhomogeneous but different kinetics and consequently different cross-linking degrees.

Moreover, the differences in the fluorescence intensity of the PEMs with two different concentrations are proportional to the degree of crosslinking obtained by trypan blue method. These colorimetric and fluorometric results demonstrate that genipin is a favorable cross-linking reagent for freestanding membranes based on CHIT/ALG multilayers, as it can efficiently cross-link the amino groups in chitosan even at low concentration.

Figure 3B displays the cross-linking degree of CHIT/ALG membranes upon genipin cross-linking. The cross-linking degree was calculated using a trypan blue standard curve, since

the absorbance of trypan blue changes in the presence of free amines. Thus, the absorbance of supernatant can be compared to the absorbance present by trypan blue at different concentrations. Moreover, it should be also pointed out that during the determination of free amines, it was also assumed that CHIT and ALG are present in the same amount in the PEMs. This assumption was based on the fact that a linear growth has previously been reported for such CHIT/ALG films 8, 10 and for CHI/ALG free standing membranes 25. Afterwards the cross-linking degree was determined comparing the free amines presented on CHIT/ALG membranes with the ones present on cross-linked membranes. The cross-linking degree could be varied from 27.5% to 64.2% by adjusting the genipin concentration. As expected membranes cross-linked with lower genipin concentration present a lower cross-linking degree. The control over the cross-linking density opens the possibility to tune the properties of multilayered films.

Mechanical Properties

The mechanical and viscoelastic properties of freestanding membranes were evaluated by dynamical mechanical analysis (DMA), an adequate non-destructive tool for characterizing biomaterials in test conditions that can more closely simulate the physiological environment39–41. DMA assays were performed in a hydrated environment at 37°C, allowing the assessment of the mechanical properties in more realistic conditions. The storage modulus (E'), loss modulus (E'') and loss factor ($tan\,\delta$) were recorded as a function of frequency on the developed un-modified and cross-linked freestanding membranes- see Figure 4A and 4B. The results show a slight increase in E', E'' and $tan\,\delta$ with increasing frequency. Moreover, the E' of cross-linked membranes at 1 and 5 $mg.mL^{-1}$ are significantly higher than in the native membranes (4 fold and 9 fold increase, respectively). All together, the results show the effective stiffening of the membranes due to genipin crosslinking. In all the formulations, no evident variation of E' was seen along the frequency axis. The $tan\,\delta$ is the ratio between the energy lost by viscous mechanisms and the energy stored in the elastic component40, 42. The $tan\,\delta$ values of all the formulations, ranging from 0.1 and 0.3, confirm the clear viscoelastic nature of all the formulations analyzed.

The mechanical properties of these membranes were also evaluated in the wet state using an universal mechanical testing equipment (tensile mode). Figure 4C shows representative stress–strain curves for all the formulations. The results show an increase of both Young modulus (E) and ultimate tensile strength (σ_{max}) with increasing genipin concentration (Table 1). The maximum extension (ε_{max}) decreases with the increase of cross-linking concentration since the structures became more brittle.

Next, we determine whether the membranes had sufficient strength to withstand physiologic forces in other effort regimes than the tensile one. To this end, a burst strength testing was also performed to determine the maximum hydrostatic pressure membranes could withstand before failure (Figure 5A). These burst strength tests are relevant for several biomedical applications, including in the development of urinary TE grafts, stents, cardiovascular devices and for membranes covering defects. Figure 5B shows representative maximum hydrostatic pressures – piston strain curves for all the formulations. Non cross-linked membranes have a higher deformation capacity which enables the membrane to withstand

higher hydrostatic pressures, followed by the membrane cross-linked at a concentration of 1 $mg.mL^{-1}$ and finally by membranes cross-linked at 5 $mg.mL^{-1}$ (Figure 5C and 5D). These results can be explained by a decrease of toughness caused by the cross-linked of the amino groups of CHIT with the ester groups of genipin. The constructs have burst pressure values within the range of urinary tract (1 kPa to 3 kPa) and is similar to that of constructs proposed for these applications 43. However, it is expected that a higher numbers of layers may further improve the mechanical properties, as has been observed before for the resistance of polyelectrolyte multilayer capsules. Thus would allow using these membranes for other biomedical applications 44.

Permeability

The permeability of CHIT/ALG membranes to nutrients was quantified using glucose as a model molecule for permeation. Figure 6A shows the representative diffusion profiles of glucose through native and cross-linked membranes. Diffusion profiles show an initial lag phase in the receptor cell due to the time required for solute traverse the membranes 45. After this phase, as the membrane is exposed to solute on the donor side, molecules begin to diffuse into the medium and the solute concentration in the bulk liquid reached equilibrium after approximately 8 hours. A faster diffusion was observed for native membranes as compared to membranes cross-linked with genipin at 1 $mg.mL^{-1}$ and 5 $mg.mL^{-1}$. The diffusion decreases as the concentration of genipin increases since the free space between the polyelectrolytes chains decrease due to the chemical cross-linking. This leads to a decrease in the water-uptake from 243.1% ± 48.3% for native membranes to 117.5% ± 9.9% and 90.3% ± 38.6% for cross-linked membranes at 1 $mg.mL^{-1}$ and 5 $mg.mL^{-1}$, respectively. The higher water content of native membranes facilitates the permeation of water soluble molecules such as glucose 46. The permeability coefficient was determined (equation 3) in the linear permeation region of the curve, as it was shown that transport parameters can be estimated more accurately in this regime (Figure 6B) 25. The permeability coefficient of glucose decreases when the cross-linking concentration increases (Table 2). The diffusion coefficients were deduced from equation 4 and the partition coefficients from equation 5 (Table 2). The diffusion coefficient is a key parameter to estimate the mass of a solute diffusing in time through the membrane 35. As expected, it decreases with increasing cross-linking concentration. The partition coefficients are a measure of solubility in the membrane 33, 47. The partition coefficients decrease with increasing cross-linking concentration, since the membranes have lower water-uptake and, consequently, the solutes have less ability to remain trapped within the membrane 35. Conversely, the native membranes have a higher K_d value, which indicates that a binding between the solute and polymer may occur. This provides an indication that the solute is easily solubilized in the membrane phase 33. The diffusion parameter values presented by these PEMs are higher than those of chitosan membranes with similar thickness 46.

Diffusion of oxygen is essential to maintain proper viability and function of living tissues 48–52. Figure 6C and 6D show the passive transport of oxygen through the freestanding membranes. In all the conditions, the amount of oxygen ($mg.L^{-1}$) increases gradually along the time. The native membranes reach faster the plateau, which was similar to the amount of oxygen presented in PBS before the purge with nitrogen. As observed for glucose, the

permeability decreases with increasing cross-linking concentration (Figure 6E). This behavior is attributed to the higher density of the polymeric meshwork in the cross-linked membranes. When compared with glucose, all the formulations presented a higher permeability and the same happens with diffusion and partition coefficients (Table 2). The higher diffusion rate of oxygen occurs probably due to the 2.5 fold difference in molecular diameter of the two molecules, since oxygen presents 3.46 Å and glucose 8.6 Å 45, 53. This is in accordance with the inverse proportionality predicted for diffusivities through the Stokes- Einstein equation 35.These results show that cross-linking with genipin at different concentrations can tailor the diffusion of molecules through the PEMs. Moreover, it was also shown that the molecular size plays an important role in the diffusion of substances across the studied PEMs. The permeation of solutes *in vivo* in this membrane should is dependent of the thickness, configuration and architectural features, including porosity and organization/density of the isolated layers contemplated in the membranes52, 53.

Comparing the values of the oxygen diffusion to *in vivo* condition the values were similar to the ones obtained in small intestine submucosa (SIS), fascia lata membranes and alloderm. However, in these cases freestanding membranes present lower equilibration time about 250-300 minutes comparing to 500-600 minutes of SIS, fascia lata and alloderm. Regarding the diffusion coefficient values, depending on the tissues different values can be targeted. For instance, SIS presented a diffusion coefficient of $7x10^{-6}$–$2x10^{-5}$ cm^2s^{-1}, alloderm 1.9-3.1 x 10^{-5} cm^2s^{-1}, fascia lata 1.6 -4 x 10^{-5} cm^2s^{-1}, aortic valve cusps $1.06x10^{-5}$ cm^2s^{-1}, cartilage $4x10^{-6}$-$2x10^{-5}$ cm^2s^{-1} and muscle 1.8 -$2.4x10^{-5}$ cm^2s^{-1} 53. For glucose diffusion the values presented in literature for diffusion coefficient are: 6.1-9.2 x 10^{-6} cm^2s^{-1} for calcium alginate capsules, 1.4-1.9 $x10^{-6}$ cm^2s^{-1} for collagen gels and 5.7-2.8 $x10^{-6}$ cm^2s^{-1} for polysulphone derivative membranes. For biological matrices the values range from $1.6x10^{-6}$ cm^2s^{-1} (human derma) to 3.8 $x10^{-7}$ cm^2s^{-1} (islet of Langerhans)54, 55. Regarding the equilibrium time the values were comparable with the ones presented by chitosan membranes 46. However, the ability of molecules to traverse homogeneous membranes are easily than in stratified membranes whereas a higher number of barriers needs to be traverse. Through the diffusion of key limiting nutrients (i.e. glucose and O_2) it is possible to estimate the potential of freestanding multilayered membranes as potential scaffolds in TE applications.

The mechanical properties and the differences in diffusion will affect different types of tissues. For instance, the stiffening effect created by genipin induces cell adhesive properties to the membranes. With exception of soft tissues such as fascia, skin, synovial membranes, etc. all the others require higher mechanical properties. Thus, it is very important to tune the physicochemical properties of polysaccharides freestanding membranes to improve their stiffness and improve their biological performance. Additionally, especially the diffusion properties will also affect the TE application envisaged. Recent approaches in tissue engineering have led to clinical success in avascular tissues (cartilage) and 2D thin organs (skin). However, one major obstacle is the regeneration of complex, large and metabolically demanding 3D tissues due to the lack of functional vascular networks 56–59.

Biological Performance

The biological performance of the developed membranes was evaluated *in vitro* with L929 cells. Cell adhesion and morphology was studied by DAPI-phalloidin after 1 and 3 days of culture (Figure 7A). The cells seeded on native membranes poorly adhered and remained round, since the films are too soft and hydrated 25. On the other hand, the cells seeded on cross-linked membranes are well spread and anchored to the PEMs, presenting a higher percentage of area covered by cells (Figure 7B). Additionally, the cells seeded on cross-linked membranes presents a similar behavior to that observed on coverglasses control (Figure S3). In all formulations, the cell number increases along culture time and in the case of cross-linked membranes the increase is even more pronounced (Figure 7C). On cross-linked membranes, cells proliferate in dense layers, whereas on native membranes they are organized in clusters. Comparing both cross-linked membranes, it can be noticed that cells are highly spread and proliferate much faster on the membranes cross-linked at the highest concentration of genipin. These results are consistent with other studies reported in literature for other PEMs and other cell types (fibroblasts, chondrocytes, osteoblasts, chondrosarcomas, muscle cells, neurons and mesenchymal stem cells), where cross-linking also improve the adhesive character of the multilayers by increasing the stiffness of the substrate, decreasing its water content and increasing protein adsorption 7, 36, 37, 60–64. All together, these results demonstrate the important role of membrane mechanics in cell adhesive properties, which is an open and issue of wide importance.

Conclusions

Freestanding membranes of CHIT and ALG with tuned properties were obtained through cross-linking with different genipin concentrations. The results showed that cross-linking lead to a minor decrease in membrane roughness. However, properties such as diffusion, storage modulus, Young modulus, maximum hydrostatic pressure and cell adhesion could be clearly modulated. Comparing all the formulations, we conclude that native membranes presented a higher permeability to basic compounds, which is a central key for biomedical applications, but had decreased mechanical properties and a decreased cell adhesion and proliferation. The importance of an adequate diffusion of oxygen and glucose are well known *in vitro* for cell viability and *in vivo* for tissue remodeling. However, depending on the application, the membrane should also sustain the loads that will be subjected.

Supporting Information

Refer to Web version on PubMed Central for supplementary material.

Acknowledgments

The authors acknowledge the financial support by the Portuguese Foundation for Science and Technology (FCT) through the doctoral and Post-doctoral grants with the reference numbers SFRH/BD/81372/2011 (JMS) and SFRH/BPD/96797/2013 (SGC), respectively. This work was financially supported by Foundation for Science and Technology (FCT), by the project PTDC/FIS/115048/2009 and by the European Commission/FP7 programme (ERC Starting grant, GA 259370 to CP). The authors would also like to acknowledge the project novel smart and biomimetic materials for innovative regenerative medicine approaches (Ref.: RL1 - ABMR - NORTE-01-0124-FEDER-000016) co-financed by North Portugal Regional Operational Programme (ON.2 – O Novo Norte), under the National Strategic Reference Framework (NSRF), through the European Regional Development Fund (ERDF).

References

1. Jaber JA, Schlenoff JB. Curr Opin Colloid Interface Sci. 2006; 11:324–329.
2. Boudou T, Crouzier T, Ren K, Blin G, Picart C. Adv Mater. 2010; 22:441–467. [PubMed: 20217734]
3. de Villiers MM, Otto DP, Strydom SJ, Lvov YM. Adv Drug Delivery Rev. 2011; 63:701–715.
4. Detzel C, Larkin A, Rajagopalan P. Tissue Eng Part B. 2011; 17:101–113.
5. Tang Z, Wang Y, Podsiadlo P, Kotov NA. Adv Mater. 2006; 18:3203–3224.
6. Couto DS, Alves NM, Mano JF. J Nanosci Nanotechnol. 2009; 9:1741–1748. [PubMed: 19435034]
7. Hillberg AL, Holmes CA, Tabrizian M. Biomaterials. 2009; 30:4463–4470. [PubMed: 19520425]
8. Alves NM, Picart C, Mano JF. Macromol Biosci. 2009; 9:776–785. [PubMed: 19340816]
9. Martins GV, Mano JF, Alves NM. Langmuir. 2011; 27:8415–8423. [PubMed: 21639130]
10. Martins GV, Merino EG, Mano JF, Alves NM. Macromol Biosci. 2010; 10:1444–1455. [PubMed: 21125694]
11. Richert L, Arntz Y, Schaaf P, Voegel J-C, Picart C. Surf Sci. 2004; 570:13–29.
12. Ariga K, Hill JP, Ji Q. Phys Chem Chem Phys. 2007; 9:2319–2340. [PubMed: 17492095]
13. Hammond PT. AIChE J. 2011; 57:2928–2940.
14. Matsusaki M, Ajiro H, Kida T, Serizawa T, Akashi M. Adv Mater. 2012; 24:454–474. [PubMed: 22213201]
15. Costa RR, Mano JF. Chem Soc Rev. 2014; 34:3453–3479.
16. Correia CR, Reis RL, Mano JF. Biomacromolecules. 2013; 14:743–751. [PubMed: 23330726]
17. Szarpak A, Cui D, Dubreuil Fdr, De Geest BG, De Cock LJ, Picart C, Auzély-Velty R. Biomacromolecules. 2010; 11:713–720. [PubMed: 20108937]
18. Larkin AL, Davis RM, Rajagopalan P. Biomacromolecules. 2010; 11:2788–2796. [PubMed: 20815399]
19. Jiang C, Tsukruk VV. Adv Mater. 2006; 18:829–840.
20. Silva JM, Duarte ARC, Custódio CA, Sher P, Neto AI, Pinho ACM, Fonseca J, Reis RL, Mano JF. Adv Healthcare Mater. 2014; 3:433–440.
21. Sher P, Custódio CA, Mano JF. Small. 2010; 6:2644–2648. [PubMed: 20938984]
22. Silva JM, Georgi N, Costa R, Sher P, Reis RL, Van Blitterswijk CA, Karperien M, Mano JF. PLoS ONE. 2013; 8:e55451. [PubMed: 23437056]
23. Costa RR, Mano JF. Chem Soc Rev. 2014; 43:3453–3479. [PubMed: 24549278]
24. Borges J, Mano JF. Chem Rev. 2014
25. Caridade SG, Monge C, Gilde F, Boudou T, Mano JF, Picart C. Biomacromolecules. 2013; 14:1653–1660. [PubMed: 23590116]
26. Chaubaroux C, Vrana E, Debry C, Schaaf P, Senger B, Voegel J-C, Haikel Y, Ringwald C, Hemmerlé J, Lavalle P, Boulmedais F. Biomacromolecules. 2012; 13:2128–2135. [PubMed: 22662909]
27. Gaudière F, Morin-Grognet S, Bidault L, Lembré P, Pauthe E, Vannier J-P, Atmani H, Ladam G, Labat B. Biomacromolecules. 2014; 15:1602–1611. [PubMed: 24666097]
28. Sundararaghavan HG, Monteiro GA, Lapin NA, Chabal YJ, Miksan JR, Shreiber DI. J Biomed Mater Res Part A. 2008; 87A:308–320.
29. Shen W-C, Yang D, Ryser HJP. Anal Biochem. 1984; 142:521–524. [PubMed: 6549372]
30. Grotzky A, Manaka Y, Fornera S, Willeke M, Walde P. Anal Methods. 2010; 2:1448–1455.
31. Oliveira MB, Song W, Martin L, Oliveira SM, Caridade SG, Alonso M, Rodriguez-Cabello JC, Mano JF. Soft Matter. 2011; 7:6426–6434.
32. Goncalves C, Rodriguez-Jasso RM, Gomes N, Teixeira JA, Belo I. Anal Methods. 2010; 2:2046–2048.
33. He H, Cao X, Lee LJ. J Controlled Release. 2004; 95:391–402.
34. Chu L-Y, Li Y, Zhu J-H, Wang H-D, Liang Y-J. J Controlled Release. 2004; 97:43–53.
35. Liang SM, Zhang L, Xu H. J Membr Sci. 2007; 287:19–28.

36. Schneider A, Vodouhê C, Richert L, Francius G, Le Guen E, Schaaf P, Voegel J-C, Frisch B, Picart C. Biomacromolecules. 2006; 8:139–145.
37. Semenov O, Malek A, Bittermann A, Vörös J, Zisch A. Tissue Eng Part A. 2009; 15:2977–2990. [PubMed: 19320572]
38. Hwang Y-J, Larsen J, Krasieva TB, Lyubovitsky JG. ACS Appl Mater Interfaces. 2011; 3:2579–2584. [PubMed: 21644569]
39. Caridade SG, Merino EG, Alves NM, Bermudez VdZ, Boccaccini AR, Mano JF. J Mech Behav Biomed Mater. 2013; 20:173–183. [PubMed: 23466499]
40. Caridade SG, Merino EG, Alves NM, Mano JF. Macromol Biosci. 2012; 12:1106–1113. [PubMed: 22707301]
41. Malheiro VN, Caridade SG, Alves NM, Mano JF. Acta Biomater. 2010; 6:418–428. [PubMed: 19607943]
42. Mano JF. Mater Sci Eng. 2005; 25:145–152.
43. Micol LA, Ananta M, Engelhardt E-M, Mudera VC, Brown RA, Hubbell JA, Frey P. Biomaterials. 2011; 32:1543–1548. [PubMed: 21074843]
44. Correia CR, Sher P, Reis RL, Mano JF. Soft Matter. 2013; 9:2125–2130.
45. Sokolnicki AM, Fisher RJ, Harrah TP, Kaplan DL. J Membr Sci. 2006; 272:15–27.
46. Singh DK, Ray AR. J Membr Sci. 1999; 155:107–112.
47. Matsuyama H, Tamura T, Kitamura Y. Sep Purif Technol. 1999; 16:181–187.
48. Cheema U, Brown RA, Alp B, MacRobert AJ. Cell Mol Life Sci. 2008; 65:177–186. [PubMed: 17994289]
49. Cheema U, Rong Z, Kirresh O, MacRobert AJ, Vadgama P, Brown RA. J Tissue Eng Regener Med. 2012; 6:77–84.
50. McClelland RE, MacDonald JM, Coger RN. Biotechnol Bioeng. 2003; 82:12–27. [PubMed: 12569620]
51. Radisic M, Malda J, Epping E, Geng W, Langer R, Vunjak-Novakovic G. Biotechnol Bioeng. 2006; 93:332–343. [PubMed: 16270298]
52. Valentin JE, Freytes DO, Grasman JM, Pesyna C, Freund J, Gilbert TW, Badylak SF. J Biomed Mater Res Part A. 2009; 91A:1010–1017.
53. Androjna C, Gatica J, Belovich J, Derwin K. Tissue Eng Part A. 2008; 14:559–569. [PubMed: 18377199]
54. Rong Z, Cheema U, Vadgama P. Analyst. 2006; 131:816–821. [PubMed: 16802027]
55. Dembczynski R, Jankowski T. Biochem Eng J. 2000; 6:41–44. [PubMed: 10908867]
56. Cuchiara MP, Gould DJ, McHale MK, Dickinson ME, West JL. Adv Funct Mater. 2012; 22:4511–4518. [PubMed: 23536744]
57. Kaully T, Kaufman-Francis K, Lesman A, Levenberg S. Tissue Eng Part B. 2009; 15:159–169.
58. Novosel EC, Kleinhans C, Kluger PJ. Ad Drug Delivery Rev. 2011; 63:300–311.
59. Rouwkema J, Rivron NC, van Blitterswijk CA. Trends Biotechnol. 2008; 26:434–441. [PubMed: 18585808]
60. Phelps JA, Morisse S, Hindié M, Degat M-C, Pauthe E, Van Tassel PR. Langmuir. 2010; 27:1123–1130. [PubMed: 21182246]
61. Pozos Vázquez, Cm; Boudou, T.; Dulong, V.; Nicolas, C.; Picart, C.; Glinel, K. Langmuir. 2009; 25:3556–3563. [PubMed: 19275180]
62. Ren K, Crouzier T, Roy C, Picart C. Adv Funct Mater. 2008; 18:1378–1389. [PubMed: 18841249]
63. Richert L, Engler AJ, Discher DE, Picart C. Biomacromolecules. 2004; 5:1908–1916. [PubMed: 15360305]
64. Schneider A, Francius G, Obeid R, Schwinté P, Hemmerlé J, Frisch B, Schaaf P, Voegel J-C, Senger B, Picart C. Langmuir. 2005; 22:1193–1200.

Europe PMC Funders Author Manuscripts

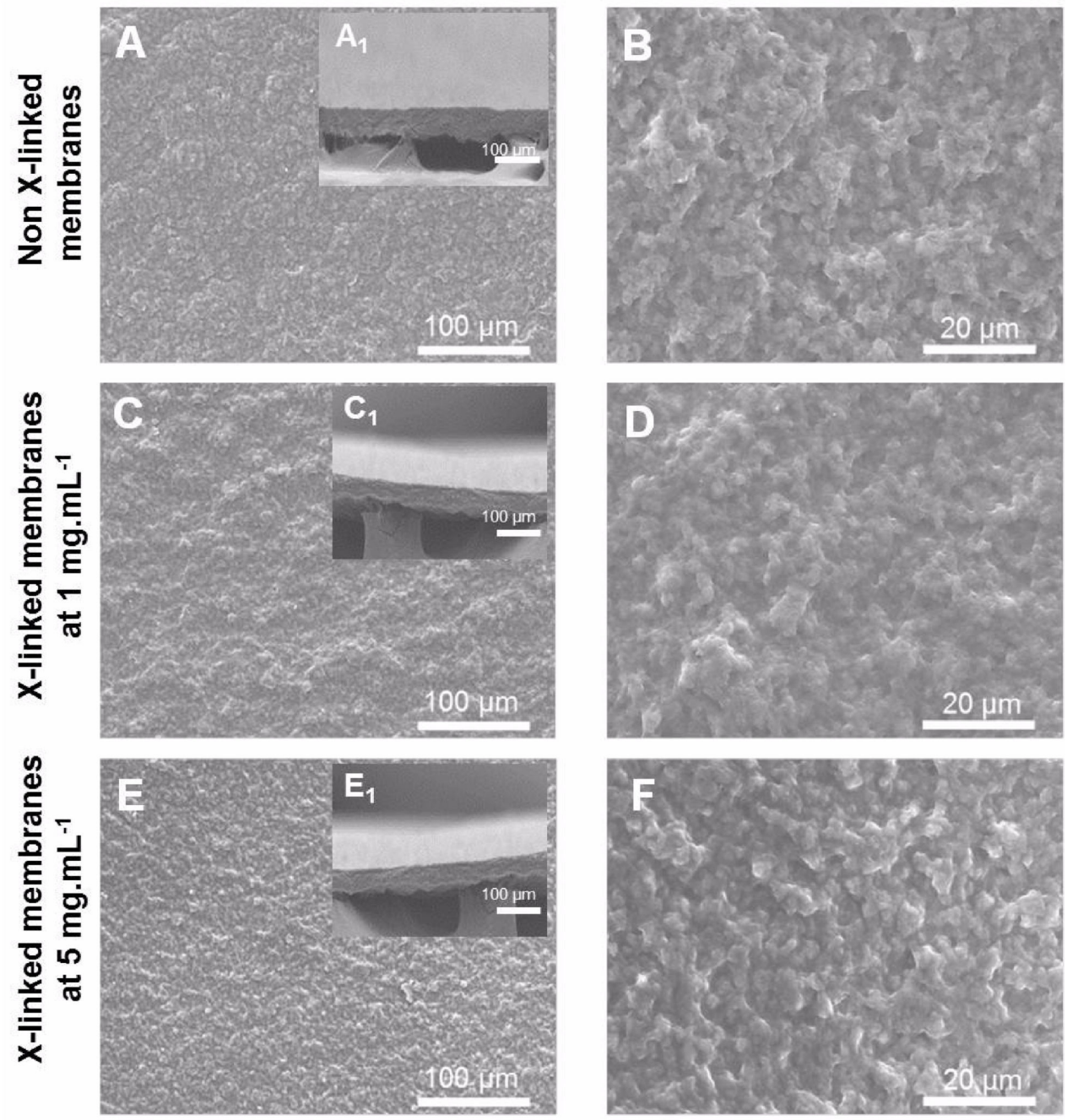

Figure 1.

Freestanding membranes morphology: SEM micrographs of the CHIT/ALG membranes (A, B) and cross-linked membranes at 1 $mg.mL^{-1}$(C,D) and 5 $mg.mL^{-1}$ (E,F) surface as well as cross-sections (inset images).

Europe PMC Funders Author Manuscripts

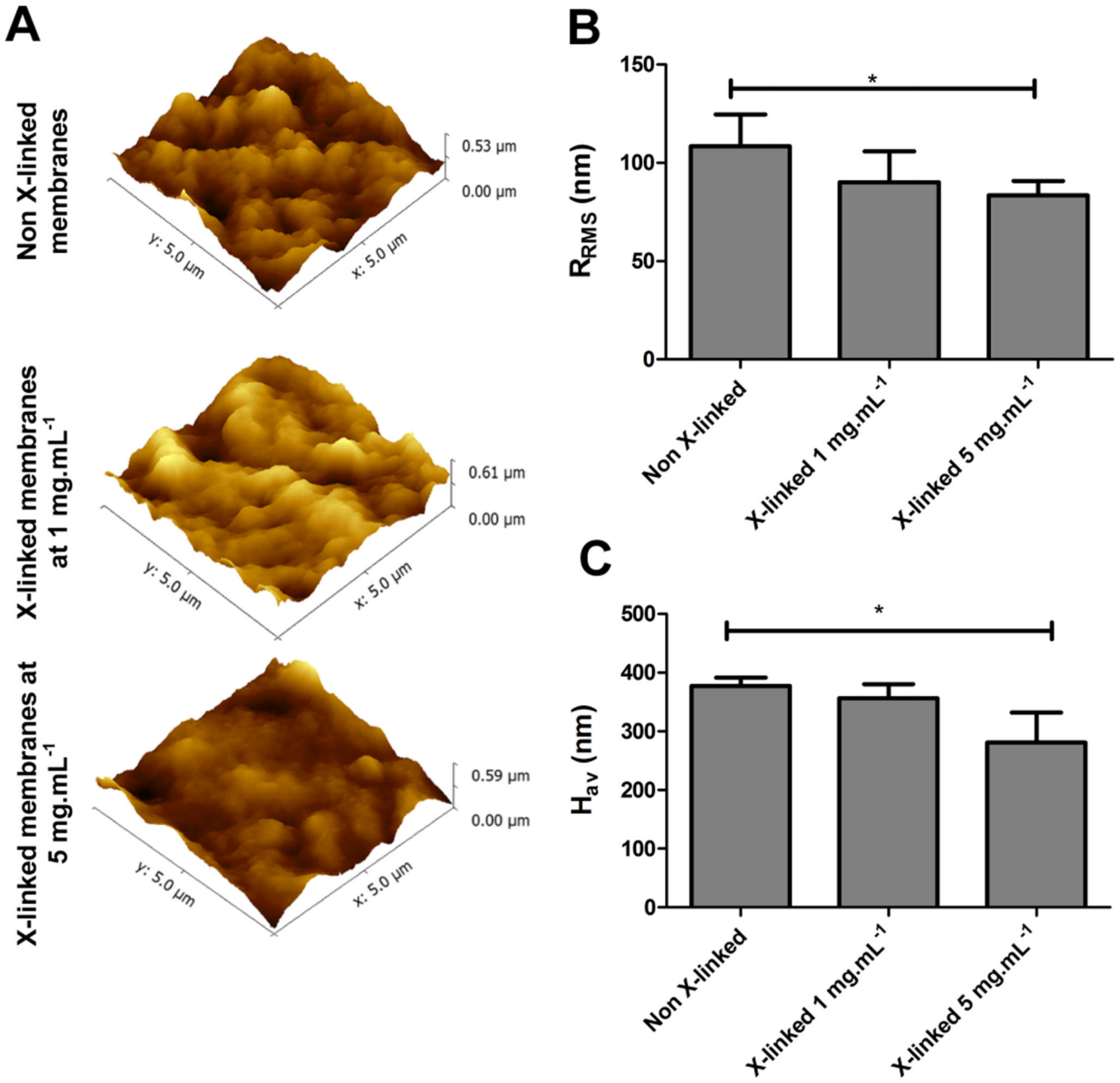

Figure 2.

Atomic force microscopy images (5×5 μm^2) of CHIT/ALG membranes without and with cross-linking (1 $mg.mL^{-1}$ and 5 $mg.mL^{-1}$) (A); Root mean squared roughness (R_{RMS}) (B) and average height value (H_{av}) (C). Significant differences were found for (*) $p < 0.05$.

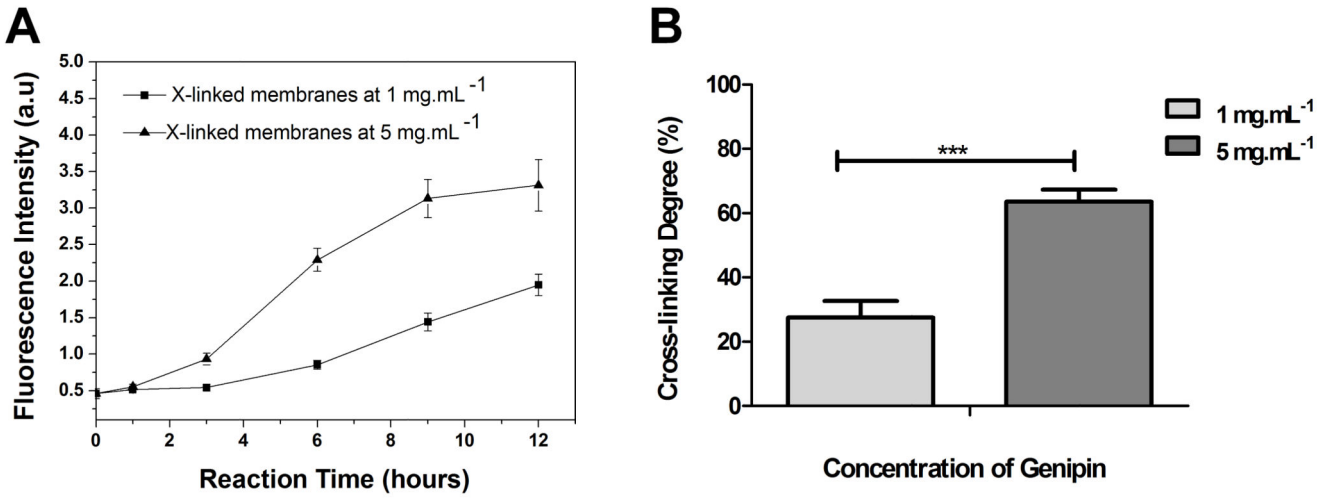

Figure 3.

Fluorometric monitoring of CHIT/ALG PEMs during cross-linked with genipin at 1 $mg.mL^{-1}$ and 5 $mg.mL^{-1}$ (A); Cross-linking degree for CHIT/ALG membranes with different genipin concentrations upon immersion for 12 hours (B). Significant differences were found for (***) $p < 0.001$.

Europe PMC Funders Author Manuscripts

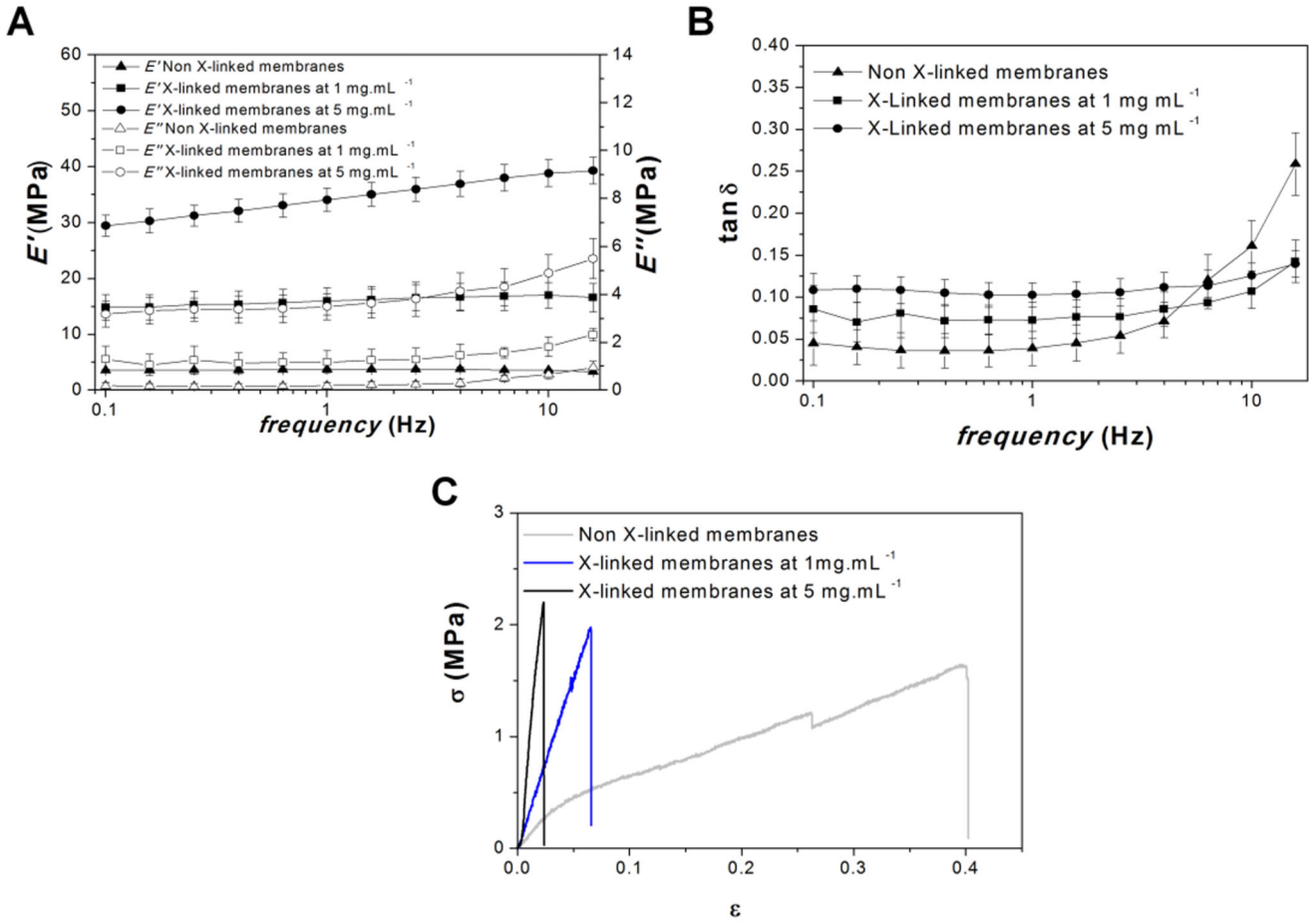

Figure 4.

Mechanical Properties: Frequency dependence of storage modulus (*E*′) and loss modulus (E") (A) and loss factor (tan δ) (B) of the freestanding membranes with and without cross-linking at 37ºC with the samples immersed in PBS. Representative tensile strain (σ)-stress (ε) curves for freestanding membranes with and without cross-linking in the wet state, after immersion in PBS solution (C).

Europe PMC Funders Author Manuscripts

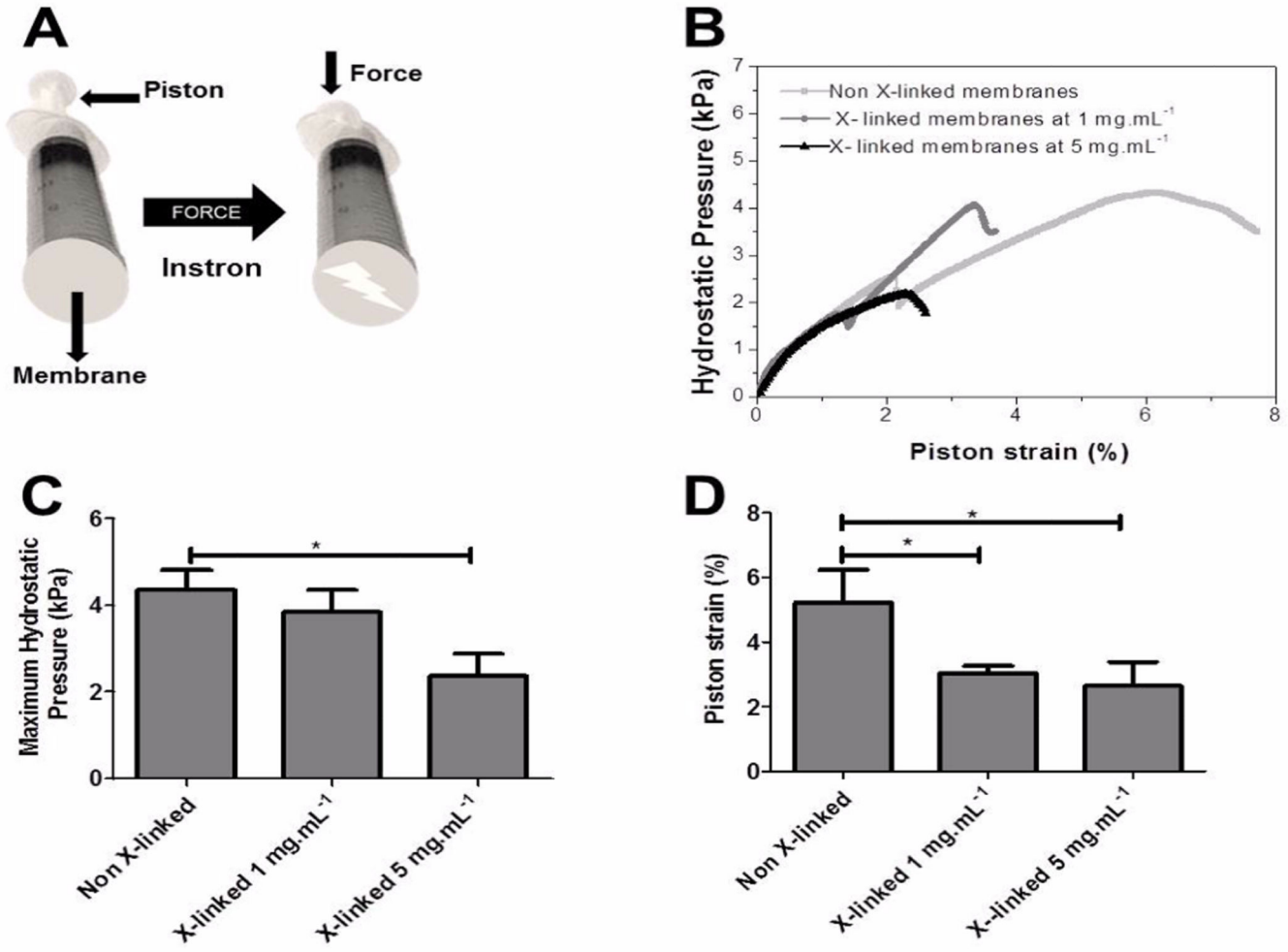

Figure 5.

Schematic representation of the home-made apparatus used to measure burst strength (A), Representative hydrostatic pressure-strain curves for CHIT/ALG membranes without and with cross-linking (1 $mg.mL^{-1}$ and 5 $mg.mL^{-1}$) (B), maximum hydrostatic pressure (C) and piston strain (D) of all the formulations. Significant differences were found for (*) $p < 0.05$.

Europe PMC Funders Author Manuscripts

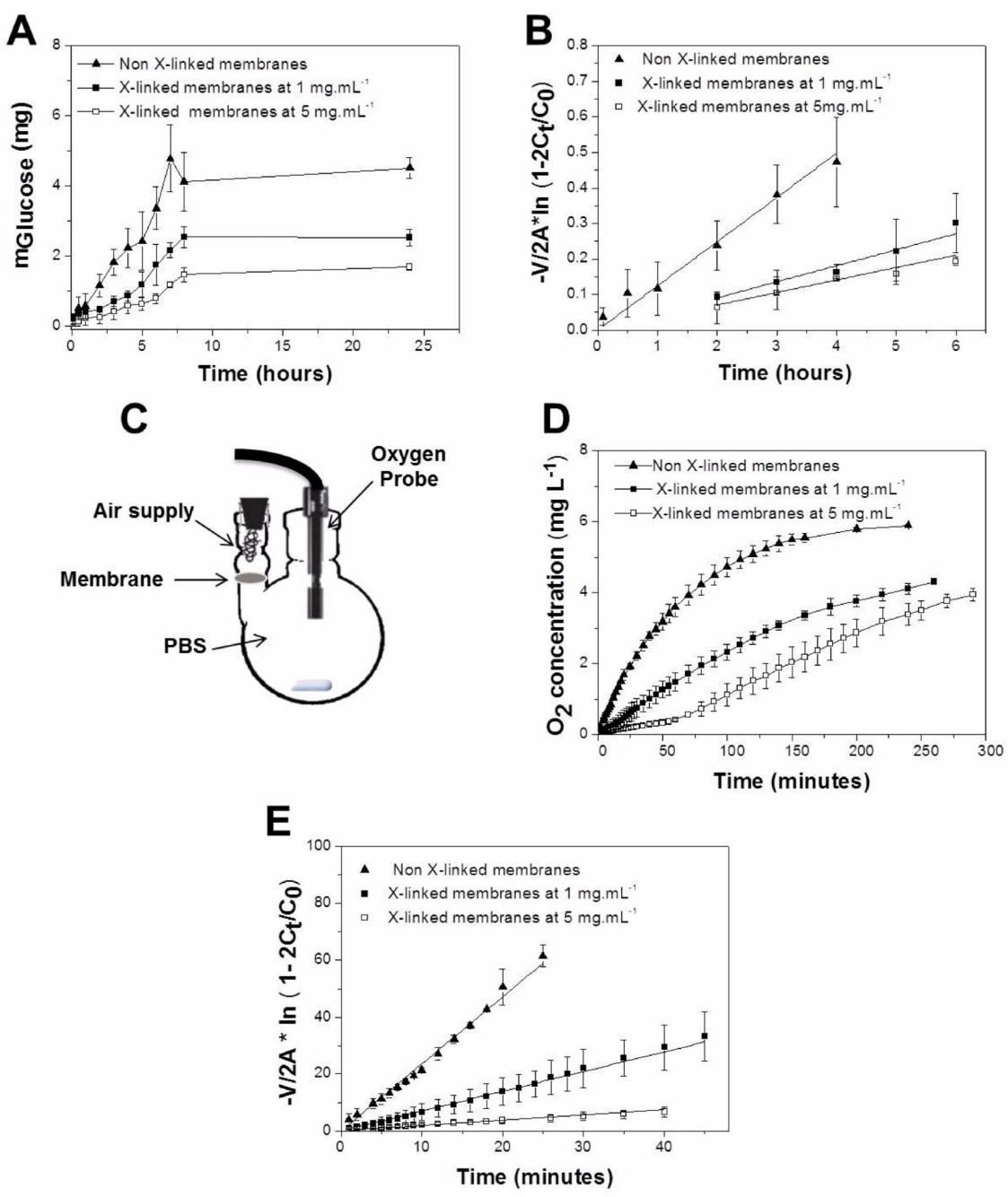

Figure 6.

Diffusion of glucose across CHIT/ALG membranes – non X-linked, cross-linked (X-linked) membranes (1 mg.mL^{-1} and 5 mg.mL^{-1}) during 24 hours at 37ºC (A). Permeation of glucose through the different membrane formulations (B). Schematic representation of the experimental oxygen diffusion system (C). Representative data of oxygen concentration levels over time within the receiver compartment for he different membrane types (D). Permeation of oxygen through the different membrane formulations (E).

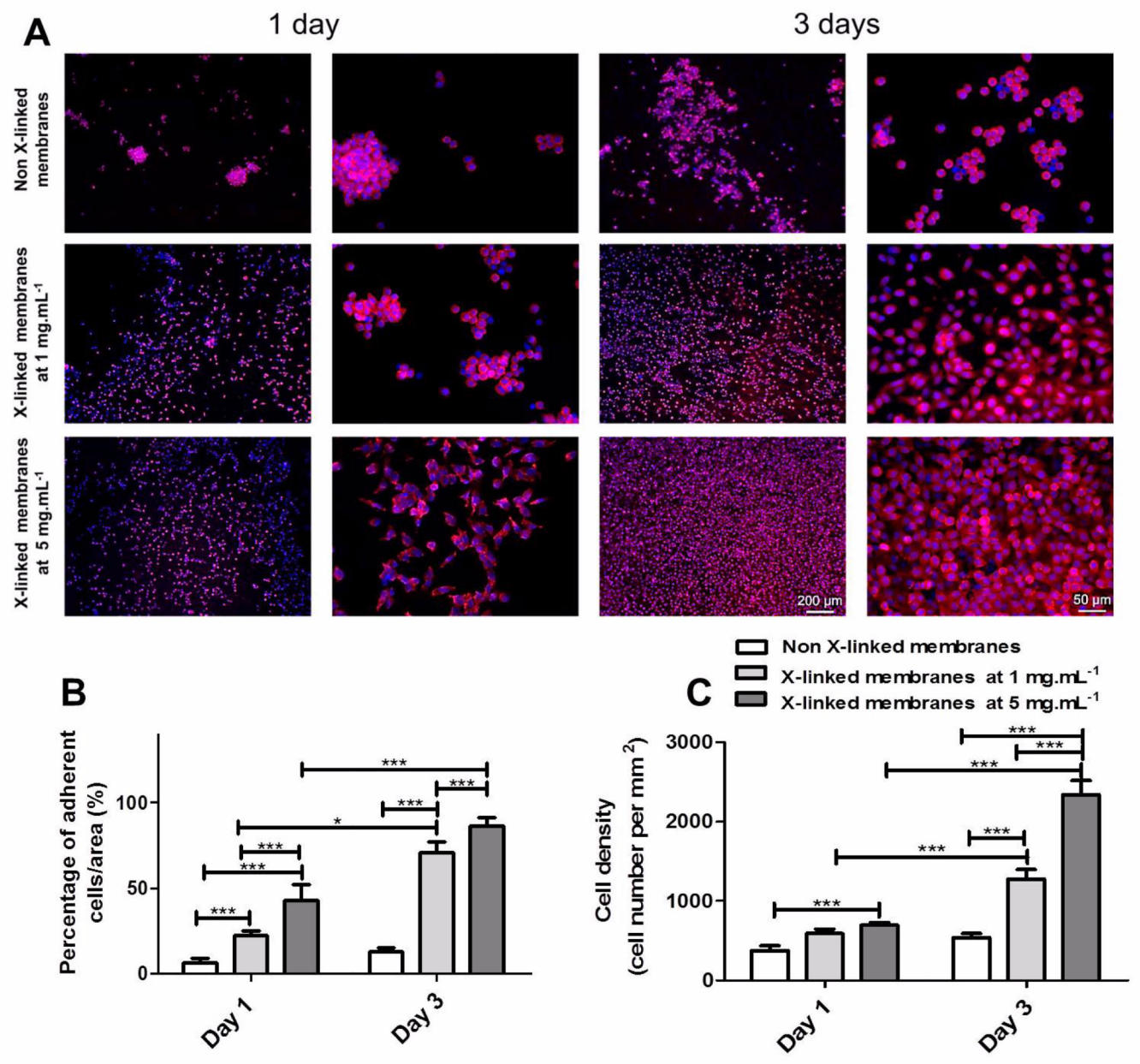

Figure 7.

DAPI-phalloidin fluorescence assay at 1 and 3 days of culture on CHIT/ALG membranes with or without cross-linking. Cells nuclei were stained blue by DAPI and F-actin filaments in red by phalloidin. Two magnifications are shown for each situation. Scale bar represents 200 µm and 50 µm in lower and higher magnification images, respectively (A). Percentage of adherent L929 per area (B) and cell density (C) after 1 and 3 days of culture on CHIT/ALG membranes without or with cross-linking (1 mg. mL^{-1} and 5 $mg.mL^{-1}$). Significant differences were found for (***) $p < 0.001$ and (*) $p<0.05$.

Europe PMC Funders Author Manuscripts

Table 1

Ultimate tensile strength (σ_{max}), maximum extension (ε_{max}) and Young modulus (E) for CHIT/ALG membranes and for cross-linked CHIT/ALG membranes in genipin solutions of 1 mg.mL^{-1} and 5 mg.mL^{-1}.Stastical analysis was performed and data was considered statistical different for p values < 0.05. (*) denote significant differences when compared to all the others cross-linking concentrations; (#) denote significant differences when compared to a cross-linking concentration of 5 mg.mL^{-1}; ($) denote significant differences when compared to a cross-linking concentration of 1 mg.mL^{-1}.

Cross-linker Concentration (mg.mL^{-1})	E (MPa)	σ_{max} (MPa)	ε_{max}
0	4.8 ± 0.8 *	1.4 ±0.2 #	0.4 ± 0.1 $+
1	12.8 ± 2 *	1.6 ± 0.4 #	0.1 ± 0.01
5	56.4 ± 6.9 *	3 ± 0.7	0.06 ± 0.003

Table 2

Permeability (*P*), partition (K_d) and diffusion (*D*) coefficients of glucose and oxygen on CHIT/ALG membranes without or with cross-linking (1 $mg.mL^{-1}$ and 5 $mg.mL^{-1}$). Stastical analysis was performed and data was considered statistical different for p values < 0.05. (*) denote significant differences when compared to all the others cross-linking concentrations; (#) denote significant differences when compared to a cross-linking concentration of 5 $mg.mL^{-1}$; ($) denote significant differences when compared to a cross-linking concentration of 1 $mg.mL^{-1}$.

	Glucose			*Oxygen*		
Cross-linker Concentration ($mg.mL^{-1}$)	***P*** **(10^{-5} cm/s)**	***D*** **(10^{-7} cm^2/s)**	K_d	***P*** **(10^{-5} cm/s)**	***D*** **(10^{-7} cm^2/s)**	K_d
0	3.7 ± 0.2*	1.9 ± 0.4#	0.55 ± 0.1	84.3 ± 5.8*	5.8 ± 0.9#$	4.2 ± 0.3#
1	1.6 ± 0.3*	1.5 ± 0.04#	0.3 ± 0.1	20.7 ± 5.1*	2.7 ± 0.1#	2.4 ± 0.7
5	0.8 ± 0.1*	0.8 ± 0.01	0.4 ± 0.03	4.8± 0.7*	1.3 ± 0.4	1.3 ± 0.6